ELSEVIER

International Journal of Heat and Fluid Flow 19 (1998) 629–635

International Journal of HEAT AND FLUID FLOW

Experimental and theoretical studies of convective heat transfer in a cylindrical porous medium

M.R. Izadpanah [a,*], H. Müller-Steinhagen [a], M. Jamialahmadi [b]

[a] *Department of Chemical and Process Engineering, The University of Surrey, Guildford, Surrey, GU2 5XH, UK*
[b] *The University of Petroleum Industry, Ahwaz, Iran*

Received 4 December 1997; accepted 30 April 1998

Abstract

Convective heat transfer at constant heat flux through unconsolidated porous media has been studied both experimentally and theoretically. Heat transfer measurements have been performed for convective heat transfer over a wide range of operational parameters at constant heat fluxes. In addition to heat transfer coefficients, pressure drop and temperature profiles both in radial and axial direction have been recorded. The equations of motion and energy which account for the non-Darcian effect are used to describe the flow and convective heat transfer through the porous medium. Mathematical models for the prediction of heat transfer coefficients and temperature profiles are presented which predict the experimental data with good accuracy.

Notation

a_e	effective thermal diffusivity, m^2/s
C	inertia coefficient
c_{pf}	fluid heat capacity, J/kg K
g	gravitational constant, m/s^2
K	permeability, m^2
p	pressure, Pa
q	heat flux, W/m^2
R_0, r_0,	radii of the bed, m
R, r,	radii, m
s	distance between thermocouple in the wall and inner surface, m
T	temperature, K
T_c	centre temperature, K
T_{TC}	thermocouple temperature, K
T_s	surface temperature, K
T_b	bulk temperature, K
T_0	initial temperature, K
u_D	Darcian velocity, m/s
Nu	Nusselt number
Pe	Peclet number
Pr	Prandtl number
Ra	Raleigh number
Re	Reynolds number
α_e	effective thermal diffusivity, m^2/s
β	coefficient of thermal expansion, K^{-1}
δ	porosity, dimensionless
Λ	separation constant
θ	dimensionless temperature
λ_e	effective thermal conductivity, W/m K
λ	thermal conductivity, W/m K
ρ_f	fluid density, kg/m^3
ρ_0	fluid density at reference temperature, kg/m^3
ρ_s	sand density, kg/m^3

1. Introduction

In the last decade there has been a steady effort to improve our knowledge of natural and forced convective heat transfer in porous media. Intensive studies, both experimental and theoretical have been performed which are reviewed by several investigators (Tien and Vafai, 1990; Stankiewicz, 1989). Among the studies carried out, convective heat transfer in saturated porous media has a special attractiveness, as a result of its wide range of applications such as chemical catalytic reactors, oil exploration, thermal insulation, geothermal operation and ground water pollution. Most of the work considered the flow to be Darcian; however, some of the researchers have extended their work to non-Darcian flow (Vafai and Tien, 1981; Hunt and Tien, 1988). Several studies concentrate on property variations of the bed such as porosity and their effect on the heat transfer process (Vafai et al., 1985). The effect of natural convection has been taken into consideration by Tien and Hunt (1987). A comprehensive review of these investigations can be found in the recently published book by Bejan and Nield (1992).

However, most of the previous investigations have been carried out with a constant wall temperature. The information

* Corresponding author. E-mail: hms@surrey.ac.uk.

0142-727X/98/$ – see front matter
PII: S0142-727X(98)10035-8

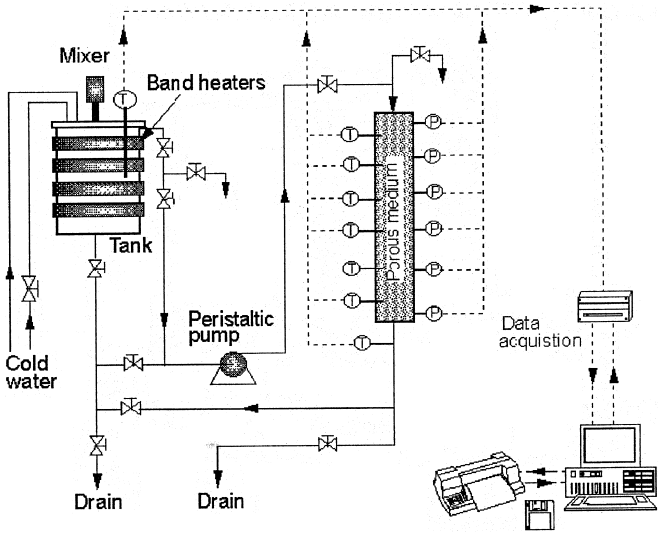

Fig. 1. Porous medium test apparatus.

published on convective heat transfer in saturated porous media under constant heat flux is scarce, specially when the flow is not fully developed. The aim of the present investigation is to study systematically the mechanism of heat transfer in a cylindrical porous medium under constant heat flux by measuring the pressure and temperature gradients along the bed and the heat transfer coefficient over a wide range of flow rate, bulk temperatures and heat flux. The equations of motion and energy are introduced in their averaged form which include the non-Darcian terms. The validity of Darcian flow is examined by solving the non-dimensionalized form of the momentum equation numerically. The volume-averaged energy equation is also solved with appropriate boundary conditions to yield a model for the prediction of the temperature profiles and heat transfer coefficients in cylindrical unconsolidated porous media. Finally, the presented model is verified against experimental data.

2. Experimental equipment and procedure

2.1. Test rig

Fig. 1 shows the test apparatus used in the present investigation. The liquid flows in a closed loop consisting of a temperature controlled tank, a pump and the test section. The tank is made of stainless steel and has a volume of about 10 litres. The temperature of the liquid in the tank is regulated by an electronic temperature controller and a variable transformer in conjunction with four band heaters covering the complete cylindrical outer surface of the tank. The liquid was pumped through the porous medium via an accurate peristaltic pump. It is capable of delivering minimum and maximum flows of 1 and 200 cm^3/min respectively, and pressures up to 3 bar. The liquid flow can be accurately controlled by varying the pump speed which is displayed on a digital screen.

The porous medium test section is a 41.5 cm long, externally heated pipe with an inside diameter of 3.2 cm. Heating is achieved by a Thermocoax heating wire which is placed in a spiral groove around the pipe and embedded by high temperature soldering tin to ensure good contact with the pipe wall. Longitudinal grooves accommodate thermocouples measuring the wall temperatures. The bed expands above and below the heated section to ensure uniform distribution of the flow. The local temperature of the wall is measured using thermocouples, which are located close below the heat transfer surface. The ratio between the distance of the thermocouples from the heat transfer surface and the thermal conductivity of the wall materials (s/λ) was determined by calibration measurements using the Wilson plot technique. The heat transfer surface temperature can be calculated using this ratio, the heat flux and the thermocouple temperature.

$$T_s = T_{TC} - \frac{q}{\lambda/s}. \tag{1}$$

Bulk temperature and pressure drop are measured using six thermocouples and six pressure transducers which are inserted along the length of the bed. Another eight thermocouples are used to measure the wall temperature at two different positions along the bed. All measurements are fed into a data acquisition system which is connected to a desk top computer.

The liquid used in the present investigation was distilled water. Sand particles with known sizes have been used to pack the test section. The physical properties of the fluid and solid particles used in this investigation are given in Table 1.

2.2. Experimental procedure and data reduction

After the tank was filled with distilled water, the heaters were switched on to raise the temperature of the liquid to a desired value. Liquid is then pumped through the bed for about one hour to obtain a homogenous condition. Then the

Table 1
Physical properties of fluid and particles

Material	Size (μm)	K (m^2)	λ (W/m K)	ρ (kg/m^3)	c_p (kJ/kg K)
Sand	180–250	1.99×10^{-10}	5.345	2640	0.82
Water	–	–	0.615	995.7	4.179

Table 2
Range of operating parameters

Flow rate	5.121×10^{-4}–4.167×10^{-3} m/s
Heat flux	1000–5000 W/m^2
Bulk temperature	26–88°C
Inlet temperature	30°C
System pressure	1.2 bar

power supply of the porous medium test heater was switched on and kept constant at a predetermined value. The system was left to stabilize for another hour before any reading was taken. Finally, the data acquisition system was switched on to record flow rate, temperatures, pressures and heat flux. Flow rate and heat flux were varied while the bulk temperature was kept constant. The experiments were carried out in an arbitrary sequence and some experiments were repeated to check the reproducibility of the experiments, which proved to be good. The local heat transfer coefficients are defined as

$$\alpha = \frac{q}{T_s - T_c}. \tag{2}$$

The range of the experimental parameters covered in this investigation is summarized in Table 2.

3. Results and discussion

3.1. Pressure drop and velocity profile

When a fluid flows through a porous medium, the pressure drop which develops along the bed in the direction of the flow is a function of system geometry, bed voidage and physical properties of the bed and of the fluid. The velocity and pressure profiles should be known before considering the mechanism of heat transfer in the bed. The operating conditions can result in four distinct flow regimes (Dybbs and Edwards, 1984): Darcy or creeping flow, inertial flow, unsteady laminar flow and chaotic flow. In the present study, the pressure drop is measured at six different positions along the porous medium in the direction of flow over a wide range of liquid velocities. Typical measurements of pressure drop at several liquid flow rates are depicted in Fig. 2 for a constant heat flux of 1500 W/m^2. The results show that a linear relationship exists between pressure drop and the distance in the direction of flow in the bed and that the slope of these lines increases with fluid velocity.

The steady state equation for the average velocity including non-Darcian effects in a cylindrical porous medium is

$$\frac{K}{\delta}\frac{1}{r}\frac{\mathrm{d}}{\mathrm{d}r}\left(r\frac{\mathrm{d}u}{\mathrm{d}r}\right) - u + \frac{K}{\mu}(\rho g - \nabla p) - \frac{K\rho_f}{\mu}Cu^2 = 0, \tag{3}$$

where

$$C = \frac{1.75(1-\delta)}{d_p\delta^2}. \tag{4}$$

Eq. (3) can be non-dimensionalized by introducing the following variables:

$$R = \frac{r}{r_0}, \quad f = \frac{K}{r_0^2\delta}, \quad \mathrm{Re}_c = \frac{KCu_D}{v}, \quad U = \frac{u}{u_D}. \tag{5}$$

Substituting in Eq. (3) and dividing by u_D yields:

$$1 - U + \mathrm{Re}_c U^2 + \frac{f}{R}\frac{\partial}{\partial R}\left(R\frac{\mathrm{d}U}{\mathrm{d}R}\right) = 0. \tag{6}$$

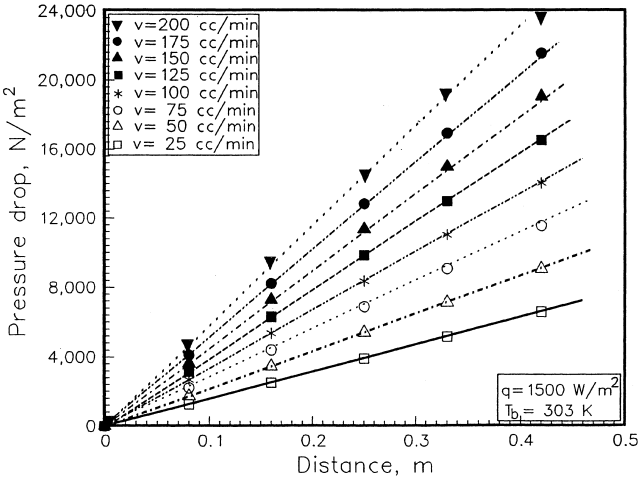

Fig. 2. Pressure drop along the porous medium.

In this investigation, the inertia term can be neglected because $\mathrm{Re}_c < 0.05$ (Tien and Hunt, 1987). Thus Eq. (6) reduces to

$$1 - U + \frac{f}{R}\frac{\partial}{\partial R}\left(R\frac{\mathrm{d}U}{\mathrm{d}R}\right) = 0. \tag{7}$$

Eq. (7) can be solved using finite difference methods. If n nodes are taken along the radius of the cylinder, then:

$$\frac{\mathrm{d}^2U}{\mathrm{d}R^2} = \frac{U_{n+1} - 2U_n + U_{n-1}}{\Delta R^2} \quad , \quad \frac{\mathrm{d}U}{\mathrm{d}R} = \frac{U_{n+1} - U_{n-1}}{2\Delta R}. \tag{8}$$

The nodal equation can be obtained from the substitution of Eq. (8) into Eq. (7)

$$\left(\frac{f}{\Delta R^2} + \frac{f}{2R_n\Delta R}\right)U_{n+1} - \left(1 + \frac{2f}{\Delta R^2}\right)U_n + \left(\frac{f}{\Delta R^2} - \frac{f}{2R_n\Delta R}\right)U_{n-1} + 1 = 0. \tag{9}$$

Boundary conditions for the solution of Eq. (7) are:

$$U = 0 \ \text{at} \ R = 1 \quad \text{and} \quad \frac{\mathrm{d}U}{\mathrm{d}R} = 0 \ \text{at} \ R = 0. \tag{10}$$

In Fig. 3 results obtained from the solution of the above finite difference equation are compared with experimental

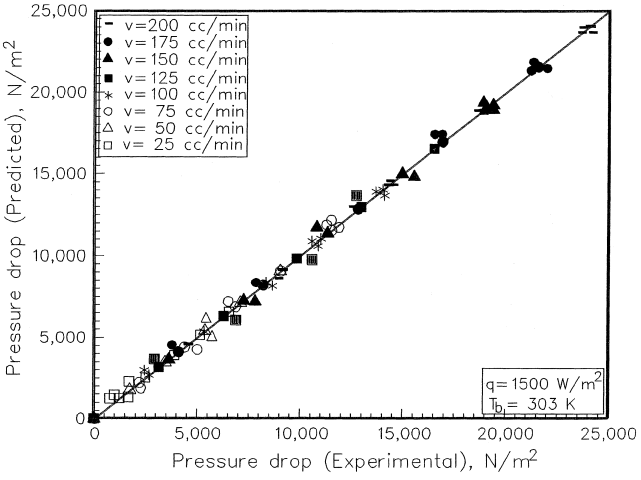

Fig. 3. Comparison of measured and predicted pressure drop.

results. Excellent agreement exists between the predictions of Eq. (7) and the experimental data. The results also revealed that when the non-Darcian term in Eq. (3) is taken into consideration only 5% improvement in the predicted results is obtained. Thus it can be assumed that the Darcian flow regime prevailed in the range of flow rates used in this investigation.

4. Heat transfer

4.1. Effect of natural convection

The effects of natural convection will have to be considered if the fluid density changes appreciably. Since the density of the fluid is a function of temperature, an equation of state is required to complement the equations of mass, momentum and energy. The simplest equation of state is (Bejan, 1984):

$$\rho_f = \rho_0[1 - \beta(T - T_0)], \tag{11}$$

where ρ_0 is the fluid density at some reference temperature T_0, and β is the coefficient of thermal expansion. In order to simplify the subsequent analysis, the Boussinesq approximation is used whenever it is valid. Applying this approximation to the Darcy model yields:

$$u = \frac{K}{\mu}\left[-\frac{dp}{dx} + \rho_0 g + \rho_0 g\beta(T - T_0)\right] \tag{12}$$

or

$$u = B' + A'(T - T_0), \tag{13}$$

where

$$A' = \frac{\rho_0 g\beta K}{\mu}. \tag{14}$$

By employing the following variables, Eq. (12) can be non-dimensionalized.

$$u_D = -\frac{K}{\mu}\left(\frac{dp}{dx} - \rho_0 g\right), \quad U = \frac{u}{u_D},$$

$$\mathrm{Ra} = \frac{kg\beta D\Delta T}{\alpha v}, \quad \mathrm{Pe} = \frac{u_D D}{\alpha}. \tag{15}$$

Substitution into Eq. (12) reduces to:

$$U = 1 + \frac{\rho_0 g\beta K}{\mu u_D}(T - T_0), \tag{16}$$

or

$$U = 1 + \frac{\mathrm{Ra}}{\mathrm{Pe}}. \tag{17}$$

The steady energy equation in a cylindrical porous medium is:

$$u\,\frac{\partial T}{\partial x} = \alpha_e \frac{1}{r}\frac{\partial}{\partial r}\left(r\,\frac{\partial T}{\partial r}\right). \tag{18}$$

Substitution of Eq. (13) in the above equation yields:

$$[B' + A'(T - T_0)]\frac{\partial T}{\partial x} = \alpha_e \frac{1}{r}\frac{\partial}{\partial r}\left(r\,\frac{\partial T}{\partial r}\right). \tag{19}$$

Eq. (19) can also be non-dimensionalized using the following variables:

$$X = \frac{2x}{r_0 \mathrm{Re}_D}, \quad x = \frac{r_0 \mathrm{Re}_D X}{2} \quad \text{hence}$$

$$\partial x = \frac{r_0 \mathrm{Re}_D}{2}\partial X, \tag{20}$$

$$\theta = \frac{k_e}{qr_0}(T - T_0), \quad T - T_0$$

$$= \frac{qr_0\theta}{k_e} \quad \text{hence} \quad \partial T = \frac{qr_0}{k_e}\,\partial\theta, \tag{21}$$

$$R = \frac{r}{r_0}, \quad r = r_0\,R \quad \text{hence} \quad \partial r = r_0\,\partial R. \tag{22}$$

Consequently, Eq. (19) reduces to

$$\left[1 + \frac{A'}{u_D}\left(qr_0\frac{\theta}{k_e}\right)\right]\frac{\partial\theta}{\partial X} = \frac{1}{\mathrm{Pr}_r}\frac{1}{R}\frac{\partial}{\partial R}\left(R\,\frac{\partial\theta}{\partial R}\right) \tag{23}$$

and with Eqs. (14) and (15) to

$$\left[1 + \frac{\mathrm{Ra}}{2\mathrm{Pe}}\theta\right]\frac{\partial\theta}{\partial X} = \frac{1}{\mathrm{Pr}_e}\frac{1}{R}\frac{\partial}{\partial R}\left(R\,\frac{\partial\theta}{\partial R}\right). \tag{24}$$

Since the value of Ra/Pe is small in the present investigation the effect of natural convection can be neglected. Fig. 4 shows that the predictions of Eq. (24) are in good agreement with the experimental observations.

Fig. 4 shows a typical variation of the heat transfer coefficient with heat flux for an inlet liquid temperature of 30°C, at two different liquid flow rates. It is obvious that the heat transfer coefficient is independent of the heat flux while it increases with liquid flow rate. Therefore, it may be concluded that the effect of natural convection is indeed negligible and that forced convection is the main mechanism of heat transfer over the range of operating conditions in this investigation. Consequently the effect of natural convection in Eq. (24) can be neglected. To perform all the experiments under identical operational conditions, the heat flux was kept constant at 1500 W/m^2 during the study of the effects of various operating parameters on convective heat transfer in the porous medium.

4.2. Axial and radial temperature profiles

Liquid enters the porous medium at a uniform temperature which is different from the wall temperature of the bed. Therefore, convective heat transfer occurs from the wall to the porous medium, and radial and axial temperature profiles begin to develop. Typical radial temperature profile obtained at constant heat flux of 1500 W/m^2 and a liquid flow rate of 100 cc/min at two different locations of the bed are shown in

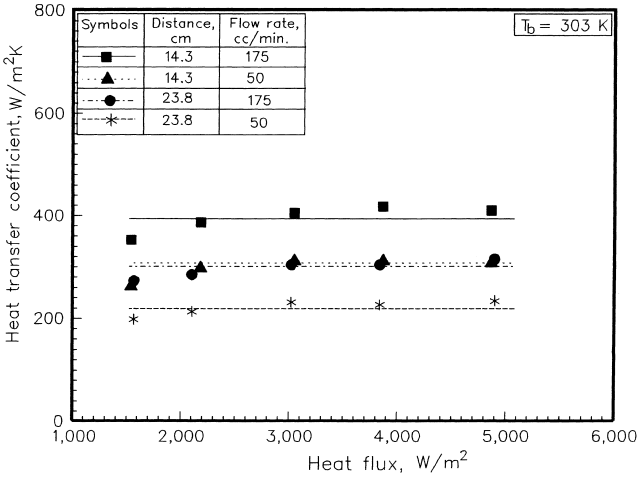

Fig. 4. Heat transfer coefficient as a function of heat flux.

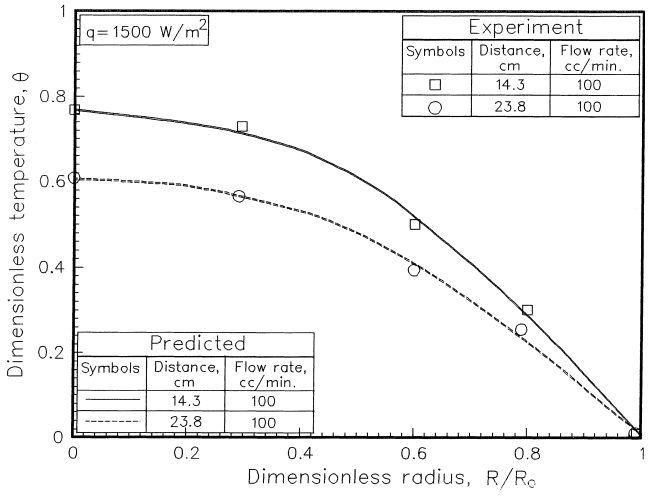

Fig. 5. Temperature distribution in radial direction.

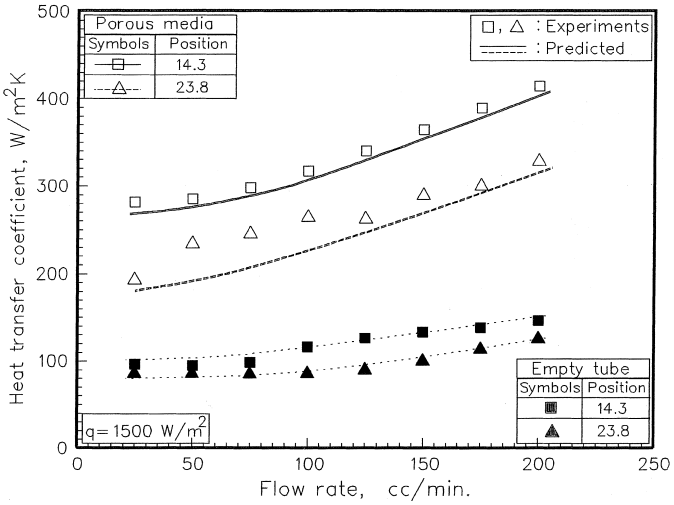

Fig. 7. Variation of heat transfer coefficient as a function of liquid flow rate.

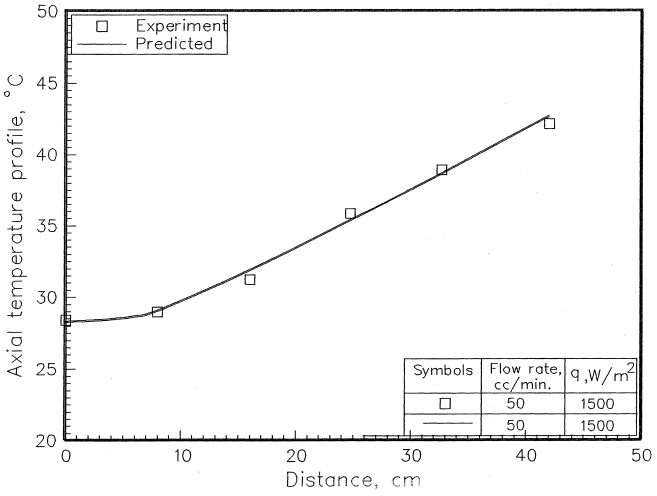

Fig. 6. Temperature distribution in axial direction.

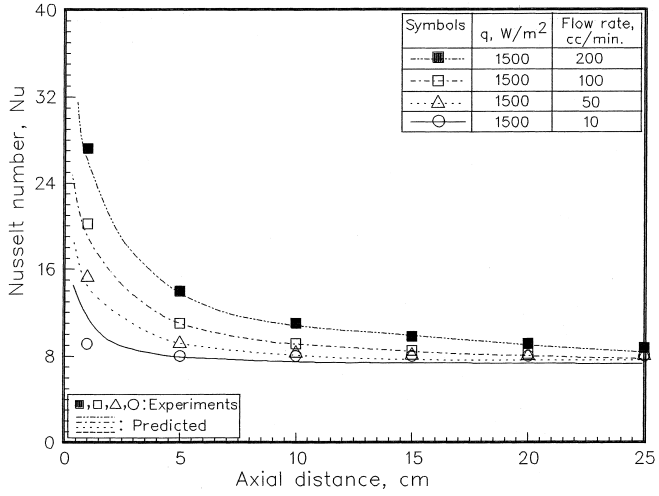

Fig. 8. Variation of Nusselt number as a function of axial distance.

Fig. 5. There is a difference of about 5°C between the wall and the centre of the bed.

The temperature gradient in the direction of flow along the central axis of the bed has also been measured. A typical axial temperature profile is depicted in Fig. 6. Heating starts at a distance of 8 cm from the bed inlet.

4.3. Heat transfer coefficient

Fig. 7 shows typical variation of the heat transfer coefficient with fluid velocity at two different locations along the bed at constant heat flux of 1500 W/m^2. For comparison, the control run for the empty tube is also included.

The results show that the convective heat transfer coefficient in the porous medium increases moderately with increasing liquid flow rate and this dependency is more pronounced at higher liquid flow rate. Furthermore, the variation of forced convective heat transfer with flow rate is more pronounced in the porous medium than in the empty tube.

Typical variations of the measured Nusselt number along the axis of the bed are shown in Fig. 8 for several different liquid flow rates. The results reveal that the temperature profile develops over a greater length as the liquid flow rate is increased. Eventually, the Nusselt number approaches a constant value of about eight for fully developed flow.

5. Formulation and modelling

5.1. Heat transfer coefficient

The volume averaged, two dimensional steady state energy equation in cylindrical coordinates is (Tien and Hunt, 1987):

$$\frac{\partial^2 T}{\partial r^2}+\frac{1}{r}\frac{\partial T}{\partial r}=\frac{u_D}{a_e}\frac{\partial T}{\partial x}-\frac{\partial^2 T}{\partial x^2}. \tag{25}$$

Eq. (25) can be non-dimensionlized using the following variables:

$$\theta = \frac{T_w - T}{T_w - T_0}, \quad r^+ = \frac{r}{r_0}, \quad x^+ = \frac{x/r_0}{\mathrm{Re}_0 \mathrm{Pr}_e}. \tag{26}$$

Thus

$$\frac{\partial^2\theta}{\partial r^{+2}} + \frac{1}{r^+}\frac{\partial\theta}{\partial r^+} = \frac{1}{2}\frac{\partial\theta}{\partial x^+} - \frac{1}{(\mathrm{Re}_0\mathrm{Pr}_e)^2}\frac{\partial^2\theta}{\partial x^{+2}}. \tag{27}$$

In the above non-dimensionlized energy equation, the last term on the right-hand side is negligible providing $\mathrm{Re}_0\mathrm{Pr}_e$ is large (Kays and Crawford, 1980). In the present investigation this condition prevails and therefore the energy equation, Eq. (27), reduces to:

$$\frac{\partial^2 T}{\partial r^2} + \frac{1}{r}\frac{\partial T}{\partial r} - \frac{u_D}{a_e}\frac{\partial T}{\partial x} = 0. \tag{28}$$

The boundary conditions of Eq. (28) in the present investigation are:

$$T_{(r,0)} = T_0, \tag{29}$$

$$\frac{\partial T}{\partial r_{(0,x)}} = 0, \tag{30}$$

$$\lambda\frac{\partial T_{(r_0,x)}}{\partial r} = q. \tag{31}$$

Analytical solution of Eq. (28) with the above boundary conditions yields:

$$T_{s_{(r_0,x)}} = T_0 + \frac{2a_e\dot{q}}{u_D\lambda_e r_0}x + \frac{\dot{q}r_0}{4\lambda_e} + \sum_{n=1}^{\infty} c_n e^{-a_e\Lambda_n^2 x/u_D} J_0(\Lambda_n r_0), \tag{32}$$

$$T_{c_{(r_0,x)}} = T_0 + \frac{\dot{q}r_0}{4\lambda_e} + \frac{2a_e\dot{q}}{u_D\lambda_e r_0}x + \sum_{n=1}^{\infty} c_n e^{-a_e\Lambda_n^2 x/u_D}, \tag{33}$$

where c_n and c_0 are

$$c_n = \frac{(2q/\lambda_e r_0\Lambda_n^2)J_2(\Lambda_n r_0)}{J_2^0(\Lambda_n r_0)}, \tag{34}$$

$$c_0 = \frac{-qr_0}{4\lambda_e}. \tag{35}$$

Therefore, the heat transfer coefficient becomes

$$\alpha = \frac{1}{\left[r_0/4\lambda_e + \sum_{n=1}^{\infty} c_n e^{-a_e\Lambda_n^2/u_D x} J_0(\Lambda_n r_0)\right]}. \tag{36}$$

Finally, the functional dependence of the Nusselt Number can be expressed as:

$$\mathrm{Nu} = \frac{2r_0}{\left[r_0/4 + \sum_{n=1}^{\infty}\lambda_e c_n e^{-a_e\Lambda_n^2 x/u_D} J_0(\Lambda_n r_0)\right]}, \tag{37}$$

Predicted and measured variation of the Nusselt number along the axis of the bed at different liquid flow rates is illustrated in Fig. 8. The calculation of the Nusselt number indicates that it approaches a constant value of eight for long beds.

A typical comparison between measured and predicted heat transfer coefficients is shown in Fig. 7 as a function of fluid velocity at constant heat flux. For comparison, the control run for the empty tube is also included. The calculated trends according to Eq. (36) are in excellent agreement with the experimental results. The applicability of the above model for heat transfer in porous media under constant heat flux is demonstrated in Fig. 9 where all the experimental data obtained for various operating conditions are compared with those predicted from Eq. (36). The absolute mean average error between measured and predicted values is 10%.

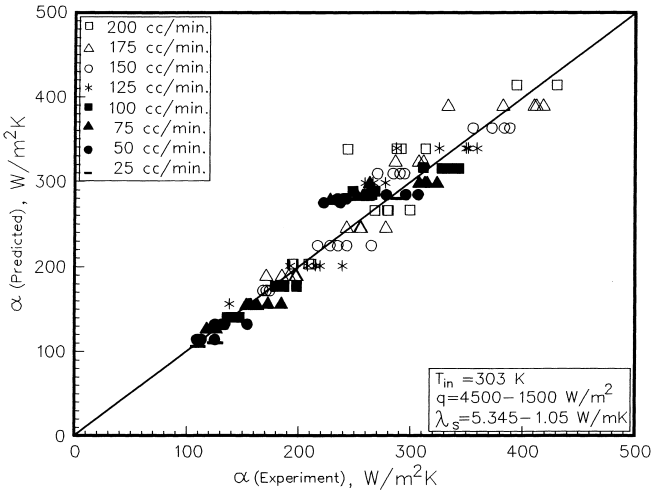

Fig. 9. Comparison of measured heat transfer coefficients with values calculated from Eq. (36).

In addition, Eqs. (32) and (33) can be used to calculate the radial and axial temperature profiles in the porous medium. These comparisons are also included in Figs. 5 and 6 for the radius and axial directions of the bed at different locations. The predicted trends are in excellent agreement with the experimental results.

6. Conclusions

The present analysis demonstrates that the Darcian assumption for the system holds and that the suggested model predicts heat transfer coefficient which compare favourably with the experimental data. It also shows that the effect of natural convection is negligible. Some of the discrepancies between theoretical and experimental values are due to the fact that the thermal conductivity of the sand was determined experimentally. However, the error between theoretical and experimental data was only about 10%.

References

Bejan, A., Nield, D.A., 1992. Convection in Porous Media. Springer, New York.

Bejan, A., 1984. Convection Heat Transfer. Wiley, New York.

Dybbs, A., Edwards, R.V., 1984. A new look at porous media fluid mechanics – Darcy to turbulent. In: Bear, Corapeioglu (Eds.), Fundamentals of Transport Phenomena in Porous Media. Martinus Nijhoff, Dordrecht, pp. 199–254.

Hunt, M.L., Tien, C.L., 1988. Non-Darcian convection in cylindrical packed beds. J. Heat Transfer 110, 378–384.

Kays, W.M., Crawford, M.E., 1980. Convective Heat and Mass Transfer. McGraw-Hill, New York.

Stankiewicz, A., 1989. Advanced modelling and design of multitubular fixed-bed reactor. Chem. Eng. Technol. 12, 113–130.

Tien, C.L., Hunt, M.L., 1987. Boundary-layer flow and heat transfer in porous beds. Chem. Eng. Process. 21, 53–63.

Tien, C.L., Vafaie, K., 1990. Convective and radiative heat transfer in porous media. Advances in Applied Mech. 27, 225–281.

Vafai, K., Tien, C.L., 1981. Boundary and inertia effects on flow and heat transfer in porous media. Int. J. Heat Mass Transfer 24, 195–203.

Vafaie, K., Alkir, R.L., Tien, C.L., 1985. An experimental investigation of heat transfer in variable porosity media. J. Heat Transfer 107, 642–647.